© 1996 Nature Publishing Group http://www.nature.com/nsmb

Ras/Rap effector specificity determined by charge reversal

Nicolas Nassar[1], Gudrun Horn[1], Christian Herrmann[1], Christoph Block[1], Ralf Janknecht[2] and Alfred Wittinghofer[1]

Members of the Ras subfamily of small GTP-binding proteins have been shown to be promiscuous towards a variety of putative effector molecules such as the protein kinase c-Raf and the Ral-specific guanine nucleotide exchange factor (Ral-GEF). To address the question of specificity of interactions we have introduced the mutations E30D and K31E into Rap and show biochemically, by X-ray structure analysis and by transfection *in vivo* that the identical core effector region of Ras and Rap (residues 32–40) is responsible for molecular recognition, but that residues outside this region are responsible for the specificity of the interaction. The major determinant for the switch in specificity is the opposite charge of residue 31—Lys in Rap, Glu in Ras—which creates a favourable complementary interface for the Ras–Raf interaction.

[1]Max-Planck-Institut für molekulare Physiologie, Abteilung Strukturelle Biologie, Postfach 102664, 44026 Dortmund, Germany
[2]Medizinische Hochschule Hannover, Institut fur molekulare Biologie, D-30623 Hannover, Germany

Correspondence should be addressed to A.W.

The crystal structure of human Rap1A (residues 1–167) in the GTP analogue form complexed with the Ras-binding domain (RBD) of the Ser/Thr specific protein kinase c-Raf1 (residues 51-131) has recently been solved[1]. It showed that the structure of Rap1A—whose primary structure displays 50% sequence identity to Ras—is essentially undistinguishable from that of Ras. It also showed that RafRBD has the ubiquitin superfold and has the same topology as ubiquitin[2–4] and the B1 immunoglobulin binding domain of streptococcal protein G[5], although there is no apparent sequence homology between these proteins. The ubiquitin α,β roll superfold[6] family of proteins also includes 2Fe–2S ferredoxin[7].

In the structure of the Rap–RafRBD complex, an antiparallel inter-protein β-sheet is shared equally by the two proteins[1] in the same way the streptococcal protein G domain is bound to an IgG heavy chain Fab fragment[8,9]. On Cα superposition of the two complexes we find the root-mean-square deviation (r.m.s.d.) between the four β-strands that form the antiparallel sheet to be 2.4 Å. This type of protein association appears, therefore, to be a paradigm for a newly recognized type of protein–protein interaction.

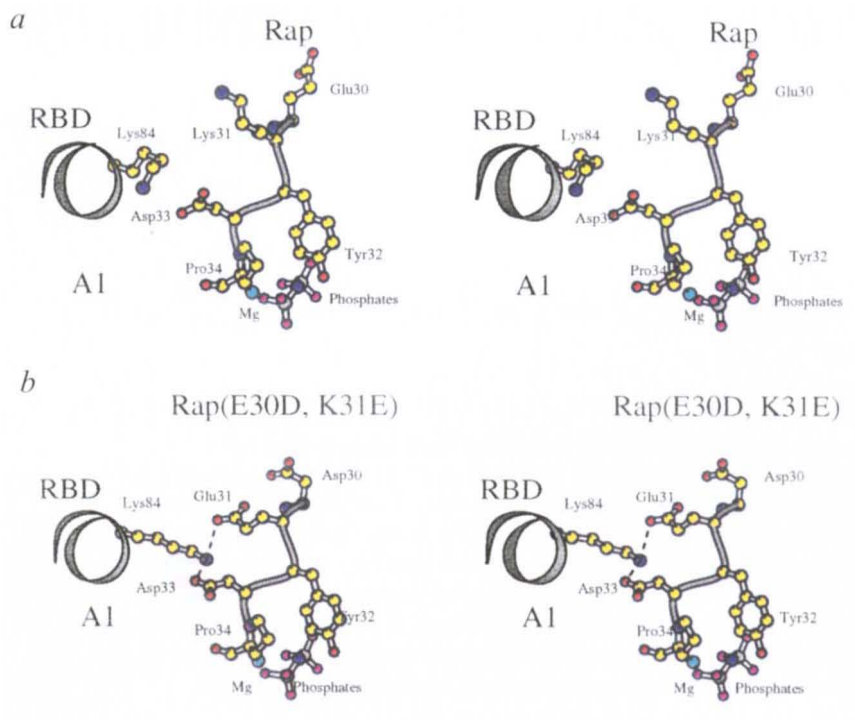
Rap1A was cloned on the basis of its sequence homology to Ras[10], or isolated as smg p21 after purification from bovine brain or human platelet membranes[11,12]. Due to the conserved sequence in the effector region it was not surprising to find that Ras and Rap bind to the same candidate effector proteins such as Raf[13], phosphatidylinositol 3-kinase (PI(3)kinase) (J. Downward, personal communication) and the exchange factor for Ral and its homologues[14–16] (termed Ral GEF, RGL, or Rlf). The interface between Rap1A and RafRBD is formed by residues 32–40 which, in Ras, have been defined genetically as constituting the effector region. This region is conserved between Rap1A and Ras and suggests that the structure of the Ras–RafRBD interface should be very similar to that of Rap–RafRBD.

However, despite these similarities, the biological activities of Ras and Rap are different, if not opposed to each other[17–20]. Whereas Ras has been found to be a central switch in many signal transduction pathways, the function of Rap1A (or any other Rap) is not known. Wheras activated Ras transforms cells, Rap1A has been cloned as a cDNA which is capable of reverting transformation induced by the K-Ras oncogene[17] and Ras-dependent activation of the Map kinase ERK[19]. Since both Ras and Rap1 have been found to interact with the same putative target molecules, there must be differences in the way the proteins interact with one another which are not detected by the two-hybrid method or other more qualitative techniques which are commonly used to demonstrate protein–protein interactions.

That Ras and Rap have different modes of interaction with their target proteins is suggested by experiments demonstrating that the affinity of the RafRBD for Ras-GTP and Rap-GTP is different by a factor of 67 (K_D=0.018 μM for Ras and 1.2 μM for Rap[21]) whereas, for the RBD from the C-terminal end of the putative effector Ral-GEF[14–16] (RGF-RBD) the affinities are reversed, with Rap1A displaying 100-fold tighter binding than Ras (ref. 21; Table 1).

Another difference between Ras and Rap relates to the finding that mutations of Lys 84 of RafRBD (K84A, K84E)—located close to the interface of the Rap1A–RafRBD complex[1]—show a decrease in affinity towards both Rap and Ras and result in the complete

© 1996 Nature Publishing Group http://www.nature.com/nsmb



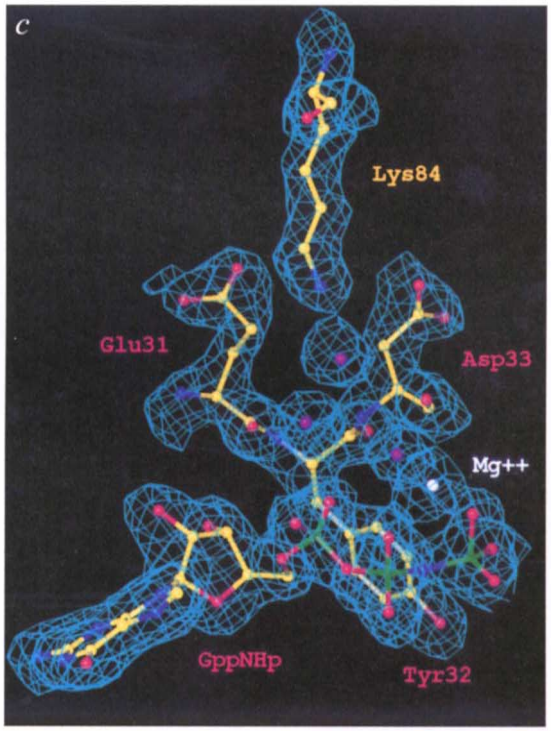


Fig. 1 Stereoimages comparing the structures of *a*, wild-type Rap/RafRBD and *b*, Rap(E30D,K31E)/RafRBD complexes indicate how the charge reversal induces a strong salt bridge of 2.8 Å between Lys 84 and Glu 31. 'A1' indicates helix A1 of the ras-binding domain ('RBD'), which bares residue Lys 84. Mg^{2+} is shown as a cyan sphere. 'Phosphates' indicates the β- and γ-phosphate portion of GppNHp. c, Final electron density map, contoured at the 1.20 σ level, around Lys 84 of RafRBD and Glu 31 in the Rap mutant calculated with $(2\boldsymbol{F}_o-\boldsymbol{F}_c)$ coefficients and model phases (image prepared with O[43]). Labels for residues of the Rap mutant are shown in red; Lys 84 of the RBD is shown in yellow. Mg^{2+} is in shown in white, and water molecules are in purple.

elimination of specificity towards either protein, whereas most other mutations of interface residues (such as K65M, R67A or N64D) show a correlated change towards Ras and Rap that retains relative differential specificity (Table 2).

These affinity measurements suggest that Lys 84 on RafRBD is more important for the Ras–Raf interaction than the Rap–Raf interaction. The Rap–Raf complex shows this lysine to be close to but not in the interface between the two proteins and near residues Glu 30, Lys 31 and Asp 33 of Rap[1] (Fig. 1*a*). On further refinement of the structure Lys 84 is observed to make a weak hydrogen bond to Asp 33 of Rap (bond length=3.5 Å), although the *B*-factor for this residue is high. Most interesting, though, is the observation that the electrostatic surface in the interface is mostly positively charged on RafRBD and mostly negatively charged on Rap1A, with the conspicuous exception of Lys 31 of Rap1A which is absent in Ras (Fig. 2). Thus, it would appear that a switch of charge at this position should generate a more complementary surface for the Ras–Raf interaction.

Mutants of Rap

Residues Glu 30 and Lys 31 of Rap1A (Asp 30 and Glu 31 in Ras) have been suggested to be partly responsible for the different biological activity of Ras and Rap1[8,22–24]. To further understand the difference between Ras and Rap in relation to their interaction with Raf we prepared mutants of Rap that resemble Ras in the effector region—such as the K31E single mutant and the (E30D, K31E) double mutant—and measured their affinities towards the effectors RafRBD and RGF-RBD. Fluorescence measurements using the GTP analogue m-GppNHp[21] show that the affinities for the interaction with RafRBD are increased to a K_D of 60 nM and 40 nM for the Rap single and double mutants, respectively—very close to the value for Ras (Table 1). The main increase in affinity is apparently due to the charge reversal on residue 31. For the RGF-RBD[16] we find the opposite effect: wild-type Rap binds the RGF-RBD 100 times more tightly than does Ras whereas the mutants weaken the interaction such that Rap's affinity now approaches that of Ras.

Rap(E30D,K31E) mutant structure

To determine the structural basis of Ras/Rap specificity, we crystallized Rap(E30D, K31E)–GppNHp bound to RafRBD and solved the structure of the complex to 2.0 Å resolution (Fig. 1*b*, *c*). The mutant complex crystallizes isomorphously with the wild-type complex and the structures of the two complexes are, in general, very similar with an overall r.m.s.d. (based on Cα superposition) of 0.83 Å. The interactions with the nucleotide analogue and the Mg^{2+} ion are matched closely in the mutant and wild-type complexes except that Tyr 32 in Rap(E30D,K31E) is coordinated to the γ-phosphate of GppNHp through a water molecule, which is contacting by hydrogen bonds the phenolic hydroxyl (bond length=2.6 Å), one phosphate oxygen (2.7 Å) and the hydroxyl of Thr 61 (2.7 Å).

© 1996 Nature Publishing Group http://www.nature.com/nsmb

The three-dimensional structure of the Rap-RafRBD complex reveals an elaborate network of mostly polar interactions between side-chain and main-chain groups—as well as a few nonpolar contacts—between the two proteins, involving many of the so-called effector residues of Ras/Rap[1]. On further refinement an additional interaction was found involving a salt bridge between the side chains of Arg 59 of RafRBD and Glu 37 of Rap1A—not observed in the structure reported[1]. The interface between the Rap double mutant and RafRBD is outlined in Fig. 3. The major difference from the previously reported wild-type interface[1], apart from changes due to the aforementioned Arg 59–Glu 37 salt bridge, are the additional interactions of Lys 84 from RafRBD which makes a tight and a weak salt bridge with Glu 31 and Asp 33, respectively, on the mutant Rap. Lys 84 also interacts with the carbonyl of Glu 31 through two water molecules (Fig 1*b*). In general, the interactions in the mutant structure are tighter, leading to lower *B*-factors.

Further, more subtle changes are also seen in the mutant complex when compared with the wild type complex. First, three loops of Rap1A containing Val 44–Gln 50, Thr 61–Met 67 and Arg 104–Val 108 each have moved by more than 1.2 Å. Second, and as in the wild-type Rap/RafRBD complex, there is a water molecule (Wat 175) located 3.54 Å from the γ-phosphorus. Wat 175 is coordinated to the backbone amide group of Gly 60 (3.1 Å) and Thr 61 (2.9 Å) and the backbone carbonyl group of Thr 35 (3.1 Å): the water has lost its coordination with the hydroxyl group of Thr 61—a feature seen in the wild-type complex—probably because of the movement of the three loops. An equivalent water molecule has been found in uncomplexed Ras–GppNHp[25] and is believed to be the attacking nucleophile of the GTPase reaction. Third, Tyr 71, (χ_1=48°) which was making a stacking interaction with Arg 68 in the wild-type complex, is now solvent exposed (χ_1=–61°).

Table 1 Change of K_D upon charge reversal[1]

	RafRBD	RGF–RBD
Ras	0.018	1.0
Rap1A	1.2	0.01
Rap(K31E)	0.06	0.15
Rap(E30D, K31E)	0.04	0.25

[1]K_Ds (in μM) of Ras, Rap, and Rap mutants for the RBDs of cRaf-1, RafRBD, and of the Ral-guanine nucleotide exchange factor, RGF-RBD.

The most remarkable feature of the mutant complex is that the average temperature (*B*-) factor has decreased by 12.4 Å^2 (13.4 Å^2 for mutant Rap and 10.9 Å^2 for RafRBD) for the main-chain Cαs relative to the wild-type complex, and the regions of high and low mobility are more-or-less conserved between the two structures, except for a few regions (for example, around Lys 31). The low *B*-factors and the better diffraction power indicate a more highly ordered crystal and/or a more rigid structure. At the same time the surface buried in the interface of the double-mutant complex as calculated using the Lee and Richards method[26,27] is increased by 4% to 1350 Å^2, and the number of close contacts (below 3.7 Å) between the two proteins is increased from 54 to 89 (I. Vetter, unpublished data), possibly due to the more intimate recognition between the two proteins as evidenced by the 30-fold increase in binding affinity. The calculated shape complementarity[28] is 0.73, similar to the wild-type complex (0.76) and the electrostatic potentials on the interacting surfaces of the mutant complex interface are now highly complementary (Fig. 2).

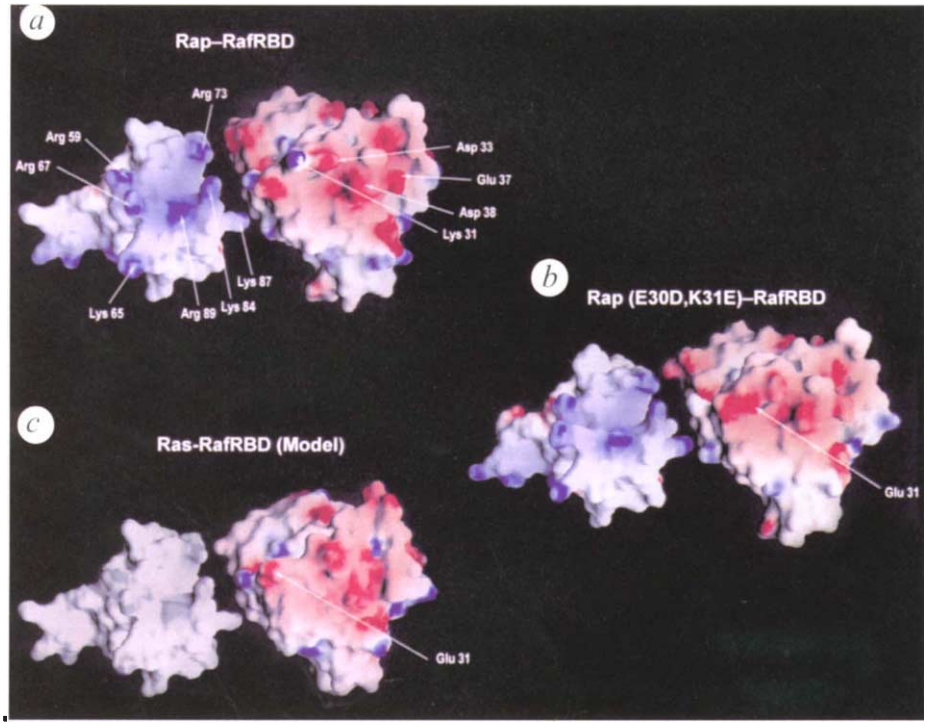


Fig. 2 Electrostatic representation of the interface of: *a*, wild-type Rap–Raf-RBD; *b*, Rap(E30D, K31E)–Raf-RBD; and *c*, Rap replaced by a model of uncomplexed Ras[25]. The components of the complex have been separated and turned towards the reader to show the interface. Figure generated using the program GRASP[47]: negative potential is coloured red and positive potential blue.

Activity *in vivo*

We have shown earlier that the affinity of the Ras–RafRBD interaction can be correlated directly to the activation of a Ras-responsive promoter *in vivo*[29]. Since the Rap double mutant has a much higher affinity towards RafRBD we tested whether it can now initiate a signalling cascade that leads to the activation of a Ras-dependent reporter gene by using a luciferase reporter gene coupled to the E74 promoter. The E74 binding site is a high affinity site for Ets transcription factors, which are activated by

© 1996 Nature Publishing Group http://www.nature.com/nsmb

Table 2 K_Ds (μM) of RafRBD mutants for Ras and Rap

c-Raf-RBD	H-Ras		Rap-1A		
mutant	K_D	(relative)	K_D	(relative)	K_D^{Rap}/K_D^{Ras}
wt	0.018	1.0	1.2	1.0	67
K65M	0.11	6.1	4	3.3	36
N64A	0.15	8.3	2.8	2.3	19
N64D	0.25	14	14.5	12	58
V69A	0.25	14	8	6.7	32
K65A	0.26	14.5	7.8	6.5	30
K65E	0.30	17	5.4	4.5	18
T68A	0.45	25	14	12	31
R67A	0.60	33	14	12	23
R59A	1.2	67	30	25	25
Q66A	1.3	72	17.3	14	13
R59A/N64D	3.8	210	125	100	33
K84A	5.0	280	11	9.2	2.2
K84E	61	3400	52	43	0.85
K84A/R89G	>100	>5000	>100	>100	–
R89L	>100	>5000	>100	>100	–

the Ras/Raf/MEK/ERK signalling pathway. Control experiments show that when a minimal, non Ras-responsive promoter is coupled to the luciferase gene, there is no induction of luciferase activity with either wild-type or mutant Rap1A (Fig. 4*b*). Transient transfection of wild-type Rap1A into RK13 cells does not lead to significant E74 promoter activation (Fig. 4*a*), whereas Rap1A(E30D, K31E) stimulates transcription sevenfold. An additional G12V mutation was then introduced into the Rap double mutant—analogous to mutations of G12 found in oncogenic Ras. Such mutations block the intrinsic, as well as the GAP-stimulated GTPase reaction of Ras[20] and Rap1A (R. Ahmadian, unpublished results). The maximum relative stimulation of Raf/MEK/ERK signalling by Rap(G12V,E30D, K31E) is 13-fold, as compared to a more than 20-fold activation measured with oncogenic Ras in our previous study[29]. However the absolute level of promoter activation was much weaker with the Rap triple mutant and, furthermore, the latter does not lead to neurite outgrowth when microinjected into PC12 cells (data not shown) whereas Ras(G12V) is a potent inducer of differentiation.

Studies with mutants in the RBD of Raf have shown that the affinity between Ras and RafRBD *in vitro* can be correlated with the increase in transcriptional activation using full-length Raf kinase *in vivo*[29]. Since the Rap(G12V) protein with the double mutation does not fit this correlation we can conclude either that other regions of Ras are involved in the Raf interaction[30,31] or that the different subcellular localization of Rap, compared to Ras, is a major factor for the different biological activities of Rap and Ras. Similar observations concerning transforming activity have been made with Ras-Rap chimeras and Rap containing multiple point mutations[18,22].

Specificity of cellular signalling

We have shown that by mutating residues 30 and 31 in Rap1A to the corresponding residues in Ras, Rap1A can interact with effector modules RafRBD and RGF-RBD in the same manner as Ras. Since we have not been able to solve the crystal structure of the Ras–RafRBD complex, and since other residues divergent between Ras and Rap1A (Fig. 5) are not located close enough to the Rap–Raf interface (residues 23/24, 26/27, 45) or whose modification is not expected to contribute to the specificity of interaction[21], we can use the high-resolution structure of the Rap mutant–RafRBD complex as a mimic of the Ras–Raf interaction. The crystal structure and the

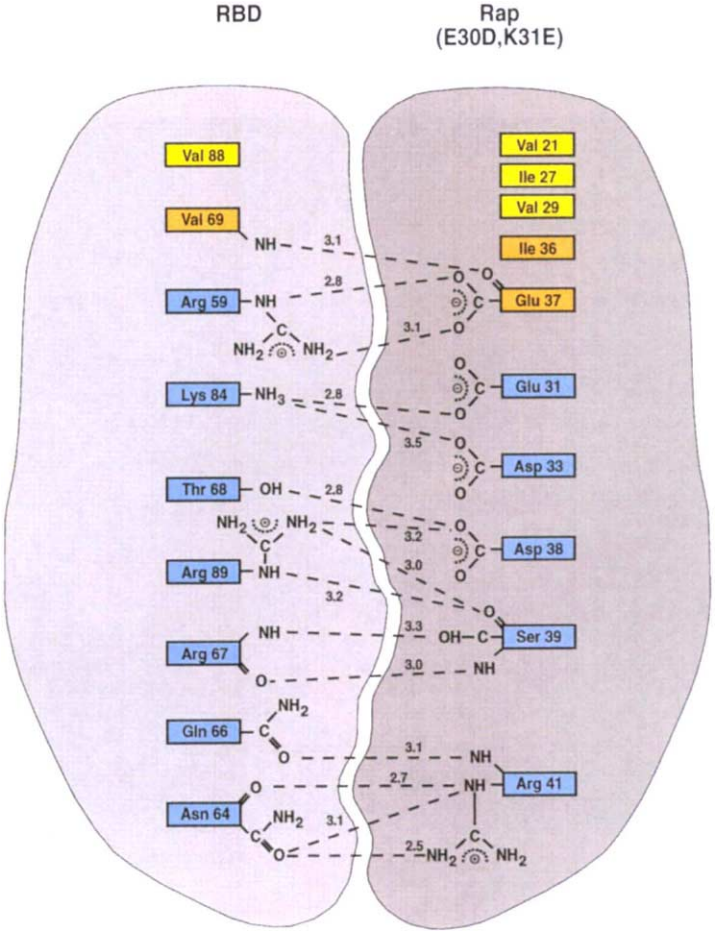


Fig. 3 Schematic view of the complex interface showing hydrogen bonds (dotted lines) and their distances. Residues involved in polar interactions are coloured blue, those in hydrophobic contacts orange (contact area 1) and yellow (contact area 2).

© 1996 Nature Publishing Group http://www.nature.com/nsmb

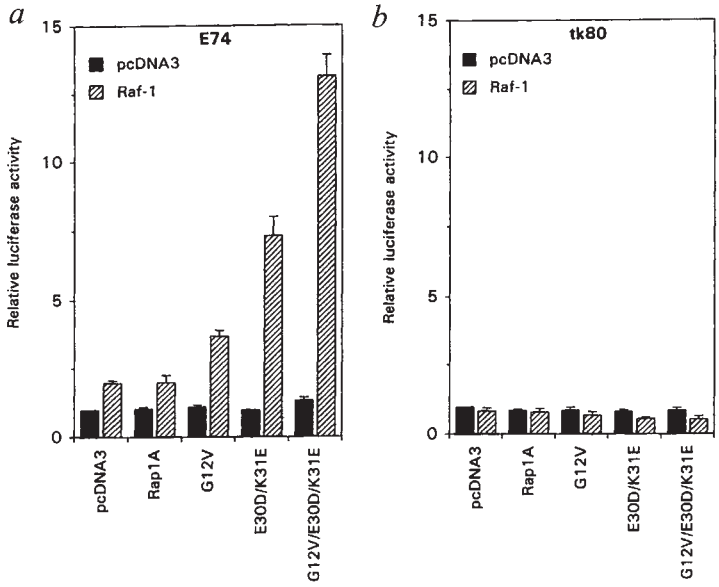


Fig. 4 *In vivo* Rap-induced transactivation in RK13 cells. *a*, Transactivation of a luciferase reporter gene induced by empty vector (pcDNA3) or vector expressing wild-type and mutant Rap1A as indicated. Transactivation was determined by measuring luminescence and normalized to β-galactosidase activity due to cotransfected pEQ176 as described previously[29]. The luciferase reporter gene is driven by a promoter containing three E74 binding sites ($E74_3$-tk80-luc) in the presence (dashed blocks) or absence of Raf (filled blocks). *b*, Analogous experiment with a luciferase reporter gene driven by a minimal promoter (tk80-luc).

biochemical experiments indicate that the difference in affinity between the two proteins for effector targets is almost exclusively due to the identity of residue 31—Lys in Rap and Glu in Ras. Exchange of Lys 31 for Glu 31 in Rap creates a more complementary surface between, and enables a favourable interaction with Lys 84 in RafRBD. This explains our earlier finding that Lys 84 is critical for Ras signalling even though it does not make any contact with Rap1A in the Rap–RafRBD complex[1,29] as well as other reports that the Ras(E31K) mutation alone or in combination with D30E inhibits Ras transformation in NIH 3T3 cells or differentiation in PC12 cells[22,24,32]. Our results also show, however, that the E30D,K31E double mutation is not sufficient to make Rap1A a good mimic of Ras in the signal transduction pathway leading to activation of the transcription factor TCF through Map kinase activation.

We and others have shown that the naturally occurring 'Ras mutants' Rap1, TC21 and R-Ras all bind to *bona fide* and putative Ras effectors such as Raf, PI(3) kinase and Ral-GEF. The sequence alignment in the effector region of members of the Ras subfamily of GTP-binding proteins shows that residues 32–40, originally defined genetically as the effector region, are more-or-less the same in Ras, Rap1 and 2, TC21 and R-Ras, but not in Ral (Fig. 5). We propose that this core effector region is a general recognition motif for the different effectors, shared by all members of the subfamily, but that residues outside of the core effector region modulate the affinity of the interaction and are thus responsible for biological specificity. From our structural studies we can speculate that binding of these effectors to members of the Ras subfamily is achieved by a common inter-protein β-sheet in a manner similar to the Ras–Raf interaction and that the specificity is determined by a few residues located outside the general recognition motif. That the interactions of one Ras subfamily GTP-binding protein with different effectors are not identical is obvious from the results of several groups, which show that the interactions of Ras with different downstream targets have different structural requirements[33–35].

Multiple effectors have also been identified for other GTP-binding proteins such as those from the Rac/Rho subfamily. These proteins also interact with their effectors at least partially through an analogous region of their polypeptide chain, since mutations of residues in this region lead to a decrease of their biological function and/or their interaction with effectors[36–39]. It will be interesting to see whether those interactions are determined by a general recognition motif—such as the antiparallel β-strand in the Ras subfamily—with additional regions of the proteins supplying specificity, as suggested by experiments involving Rac/Rho chimeras[38]. It will also be interesting to investigate whether the specificity of the interaction of Ras and Rap with their regulatory proteins GAP and GEF are dependent on similar residues in the effector site: it has been shown already that the GTPase stimulation of Ras by p120-GAP is dependent on Glu 31[24].

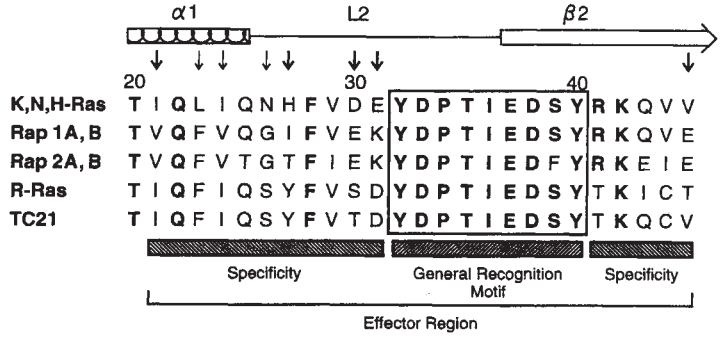


Fig. 5 Sequence alignment between proteins of the Ras subfamily of GTP-binding proteins, encompassing the region that has been implicated in effector binding[18,20–24]. A sequence that has been shown genetically as the effector region, which we call the core effector region, is almost completely conserved between members of the subfamily and is responsible for the general recognition between Rap and RafRBD[1], as well as for mediating the effector interactions of Ras, R-Ras and TC21. The region outside the general recognition motif is not conserved between the Ras subfamily members and mediates the specificity of the biological response. Of the residues that are different between Ras and Rap1 (indicated by arrows), those that are thought to be crucial for the specificity are highlighted (by thick arrows).

© 1996 Nature Publishing Group http://www.nature.com/nsmb

Methods

Cloning procedures, protein preparations. The Rap mutants were made by site-directed mutagenesis using single-stranded human Rap1A DNA from the pBKS vector with the transformer site-directed mutagenesis kit from Clontech. The mutagenic oligonucleotides were 5'–GAATTTTTGTTGAAGAATATGACCCAAC–3' for K31E and 5'–CAGGGAATTTTTGTCGACGAATATGACCCAACG–3' for the D30E, K31E double mutation. The truncated versions of Ras(1–166) and Rap1A(1–167) were prepared from ptac expression vectors as described previously[1,40]. RafRBD mutants were created from the RafRBD or the Raf regulatory region cDNA in pGEX-2T (Pharmacia) as described previously[29]. Wild-type and mutant RafRBD were expressed as GST-fusion proteins, purified using glutathione-sepharose, cleaved with thrombin and purified further as described previously[29].

Affinity measurements. Dissociation constants (in μM) for complexes of RBD's with Ras or Rap bound to the fluorescent GTP analogue mGppNHp were measured with fluorescence, by employing the GDI effect of effector binding on the dissociation of fluorescent nucleotide as described before[21,40]. Buffer conditions were: 50 mM Tris.HCl, 5 mM $MgCl_2$, 2 mM dithiothreitol, pH 7.4.

Protein crystallization. Truncated human Rap1 double mutant (E30D, K31E), residues 1–167, and RafRBD (residues 51–131) were purified as described previously[21,40] and concentrated to 20 mg ml^{-1} each before mixing in stoichiometric amounts. To remove uncomplexed components, the complex was purified by gel filtration on Superdex-75 as described previously[1]. Fractions containing Rap/RafRBD were pooled and concentrated (Amicon filtration, 10,000 M_r cutoff). Protein crystals were grown by the hanging drop method at 19 °C by equilibration against a reservoir containing 11% PEG 4000, 2 mM dithiothreitol, 80 mM Tris-HCl pH 7.6, 5 mM $MgCl_2$ and 20–50 mM calcium acetate. 4 μl of concentrated (15 mg ml^{-1}) Rap/RafRBD and 4 μl of the reservoir solution were mixed on siliconized glass coverslips. Crystals appeared after few minutes of equilibration and attained dimensions of 0.5 mm×0.5 mm×0.3 mm after 24 h. The crystals belong to the orthorombic space group $P2_12_12_1$, with one molecule in the asymmetric unit. Unit cell parameters are a=44.5, b=71.8, c=100.3 Å, isomorphous with the wild type complex crystals[1]. Solvent content of the crystals is 50%.

X-ray data collection. X-ray diffraction extended beyond 1.8 Å. Diffraction data were collected on a 3 circles Hi-Star Siemens area detector at 4 °C with graphite-monochromated CuKα X-rays generated by a Siemens generator operating at 45 kV and 100 mA. Two crystals were mounted in a glass capillary and the crystal to detector distance was set to 13 cm. Crystals were randomly positioned in the X-ray beam and images of 0.09° width were taken rotating along the vertical -axis. Images were indexed and intensities integrated using XDS[41]. Data were scaled using XSCALE (W.Kabsch) to a final resolution of 2.0 Å giving a set of 26,720 unique reflections with a final R_{sym}=4.1% calculated on intensities.

Structure determination and refinement. The complete model was refined using stereochemically restrained simulated annealing and positional refinement with X-PLOR 3.1[42], model building and electron density map inspection were carried out using the program O[43]. The structure of wild-type Rap–RafRBD[1] was initially divided into two independent groups: a wild-type Rap group containing also one GppNHp molecule and one Mg^{2+} ion and an RafRBD group containing one Ca^{2+} ion, and submitted to a rigid body refinement against data in the 8.0–2.9 Å resolution shell. This step decreased the crystallographic R-factor from 52.2 to 38.5%. Resolution was then increased in 0.1 Å steps to 2.0 Å. At each step one cycle of simulated annealing with initial temperature of 3000 K followed by 120 cycles of positional refinement with constant temperature factors (B=15) were performed. At the end of each step isotropic individual temperature factors were refined. When a resolution of 2.5 Å was reached, water molecules were manually placed in the structure. Electron density peaks were assigned to water molecules if: (i) they were present in both ($\boldsymbol{F}_o$–$\boldsymbol{F}_c$) and ($2\boldsymbol{F}_o$–$\boldsymbol{F}_c$) electron density maps; (ii) they were present at a cut-off of 4.5σ in the ($\boldsymbol{F}_o$–$\boldsymbol{F}_c$) map; (iii) they were surrounded by at least one proton acceptor/donor; and (iv), their temperature factor after refinement did not exceed 35 $Å^2$. The final model of the double mutant complex consists of Rap(1–167), RafRBD(56–131), one GppNHp, one Mg^{2+} ion, one Ca^{2+} ion and 89 water molecules. Residues 51–55 in RafRBD are disordered in the electron density map. The final crystallographic R-factor for all data (21,693 reflections) is 22.0% and 21.1% for ($\boldsymbol{F}$>2σ($\boldsymbol{F}$)) data (20,409 reflections). The r.m.s. deviations from ideal bond distances and bond angles are 0.013 Å and 1.94° respectively. A Wilson plot of the data in the 8.0–2.0 Å resolution shell gives a temperature factor of 19.3 $Å^2$. A Luzzati plot[44] gives an upper-limit error on coordinates of 0.25 Å, a σ(A) plot gives an error of <|Δr|>=0.21 Å on coordinates[45] and an average figure of merit of 0.87. Main chain φ and ψ torsion angles for 90.5% of the non-glycine residues fall within most-favoured regions of the Ramachandran plot, as defined in the program PROCHECK[46]. The main-chain and side-chain average temperature factors are 16.9 $Å^2$ and 20.5 $Å^2$ respectively. The average real-space correlation coefficient is 0.916, as calculated by O[43]. With respect to the wild-type complex, the double-mutant complex has rotated in the crystal lattice by (10.2°, –8.1°, 3.6°) and moved by (2.37 Å, 0.77 Å, –0.18 Å) as calculated by the program SUPERPOSE (CCP4), showing a significant rigid body adaptation of the two proteins upon introduction of the E30D,K31E mutations.

The r.m.s. deviation of the wild-type and the mutant Rap–RafRBD complex based on Cα superimposition was done with the program SUPERPOSE as implemented in the CCP4 program chain. The r.m.s. deviation between Rap and Rap(E30D, K31E) is 0.75 Å, and between RafRBD in the two structures is 0.99 Å.

Coordinates have been submitted to the Brookhaven Protein Data Bank. The identification (ID) code is 1GUA.

Reporter gene assays. Rabbit kidney epithelial-like RK13 cells were used for the transfection assays with the luciferase reporter gene constructs which either contain (E74-tk80-luc) or do not (tk80-luc) contain a TCF responsive promoter as described previously[29]. A β-galactosidase expression vector (pEQ176) was used for standardization of the results. Wild-type and mutant Rap cDNAs were cloned into the mammalian expression vector pcDNA3 by using the polymerase chain reaction and the bacterial ptac expression constructs. 36 h after transfection, cells were harvested and lysed and luciferase and β-galactosidase activities were determined. The relative luciferase activity was normalized to the β-galactosidase activity.

Received 6 May; accepted 27 June 1996.

© 1996 Nature Publishing Group http://www.nature.com/nsmb

Acknowledgements
We thank S.B. Wohlgemuth, B. Voss and D. Vogt for excellent technical assistance, I. Vetter and F. Schmitz for computer assistance and discussion, R. Mittal for critical reading of the manuscript, the Bayer Corporation and the Deutsche Forschungsgemeinschaft (DFG) for financial support.

1. Nassar, N. *et al.* The 2.2 Å crystal structure of the Ras-binding domain of the serine/threonine kinase c-Raf1 in complex with Rap1A and a GTP analogue. *Nature* **375**, 554–560 (1995).
2. Vijay-Kumar, S., Bugg, C.E. & Cook, W.J. Structure of ubiquitin refined at 1•8 Å resolution. *J. Mol. Biol.* **194**, 531–544 (1987).
3. Weber, P.L., Brown, S.C. & Mueller, L. Sequential ^{1}H NMR assignments and secondary structure identification of human ubiquitin. *Biochemistry* **26**, 7282–7290 (1987).
4. Di Stefano, D.L. & Wand, A.J. Two-dimensional 1H NMR study of human ubiquitin: a main chain directed assignment and structure analysis. *Biochemistry* **26**, 7272–7281 (1987).
5. Derrick, J.P. & Wigley, D.B. The third IgG-binding domain from streptococcal protein G. *J. Mol. Biol.* **243**, 906–918 (1994).
6. Orengo, C.A., Jones, D.T. & Thornton, J.M. Protein superfamilies and domain superfolds. *Nature* **372**, 631–634 (1994).
7. Tsukihara, T. Structure of the [2Fe-2S] Ferredoxin I from the blue-green Alga *Aphanothece sacrum* at 2.2 Å resolution. *J. Mol. Biol.* **216**, 399–410 (1990).
8. Derrick, J.P. & Wigley, D.B. Crystal structure of a streptococcal protein G domain bound to an Fab fragment. *Nature* **359**, 752–754 (1992).
9. Lian, L.Y., Barsukov, I.L., Derrick, J.P. & Roberts, G.C.K. Mapping the interactions between streptococcal protein G and the Fab fragment of IgG in solution. *Nature Struct. Biol.* **1**, 355–357 (1994).
10. Pizon, V., Chardin, P., Lerosey,I., Olofsson, B. & Tavitian, A. Human cDNAs rap1 and rap2 homologous to the Drosophila gene Dras3 encode proteins closely related to ras in the 'effector' region. *Oncogene* **3**, 201–204 (1988).
11. Kawata, M. *et al.* A novel small molecular weight GTP-binding protein with the same putative effector domain as the ras proteins in bovine brain membranes. *J. Biol. Chem.* **263**, 18965–18971 (1988).
12. Ohmori, T., Kikuchi, A., Yamamoto, K., Kim, S. & Takai, Y. Small molecular weight GTP-binding proteins in human platelet membranes. *J. Biol. Chem.* **264**, 1877–1881 (1989).
13. Zhang, X.-f. *et al.* Normal and oncogenic p21^{ras} proteins bind to the amino-terminal regulatory domain of c-Raf-1. *Nature* **364**, 308–313 (1993).
14. Hofer, F., Fields, S., Schneider, D. & Martin,G.S. Activated Ras interacts with the Ral guanine nucleotide dissociation stimulator. *Proc. Natl. Acad. Sci. USA* **91**, 11089–11093 (1994).
15. Kikuchi, A., Demo, S.D., Ye, Zhi-Hai, Chen, Y.-W. & Williams, L.T. RalGDS family members interact with the effector loop of *ras* p21. *Mol. Cell. Biol.* **14**, 7483–7491 (1994).
16. Spaargaren, M. & Bischoff, J.R. Identification of the guanine nucleotide dissociation stimulator for Ral as a putative effector molecule of R-ras, H-ras, K-ras, and Rap. *Proc. Natl. Acad. Sci. USA* **91**, 12609–12613 (1994).
17. Kitayama, H., Sugimoto, Y., Matsuzaki, T., Ikawa, Y. & Noda, M. A *ras*-related gene with transformation suppressor activity. *Cell* **56**, 77–84 (1989).
18. Zhang, K., Noda, M., Vass, W.C., Papageorge, A.G. & Lowy, D.R. Identification of small clusters of divergent amino acids that mediate the opposing effects of ras and Krev-1. *Science* **249**, 162–165 (1990).
19. Cook, S.J., Rubinfeld, B., Albert, I. & McCormick, F. RapV12 antagonizes Ras-dependent activation of ERK1 and ERK2 by LPA and EGF in Rat-1 fibroblasts. *EMBO J.* **12**, 3475–3485 (1993).
20. Marshall, M.S.The effector interactions of p21^{ras}. *Trends Biochem. Sci.* **18**, 250–254 (1993).
21. Herrmann, C., Horn, G., Spaargaren, M. & Wittinghofer, A. Differential interaction of the Ras family GTP-binding proteins H-Ras, Rap1A and R-Ras with the putative effector molecules Raf-kinase and Ral-guanine nucleotide exchange factor. *J. Biol. Chem.* **271**, 6794–6800 (1996).
22. Marshall, M.S. *et al.* Identification of amino acid residues required for ras p21 target activation. *Mol. Cell. Biol.* **11**, 3997–4004 (1991).
23. Zhang, K. *et al.* Heterogeneous amino acids in ras and rap1A specifying sensitivity to GAP proteins. *Science* **254**, 1630–1634 (1991).
24. Shirouzu, M. *et al.* A glutamic acid residue at position 31 of Ras protein is essential to the signal transduction for neurite outgrowth of PC12 cells and the stimulation of GTPase activity by GAP^{RAS}. *Oncogene* **7**, 475–480 (1992).
25. Pai, E.F. *et al.* Refined crystal structure of the triphosphate conformation of H-*ras* p21 at 1.35Å resolution: implications for the mechanism of GTP hydrolysis. *EMBO J.* **9**, 2351–2359 (1990).
26. Lee, B. & Richards, F.M. The interpretation of protein structures: estimation of static accessibility. *J. Mol. Biol.* **55**, 379–400 (1971).
27. Programs for Protein Crystallography. *Acta Crystallogr.* D**50** 760–763 (1994).
28. Lawrence, M.C. & Colman, P.M. Shape complementarity at protein/protein interfaces. *J. Mol. Biol.* **234**, 946–950 (1993).
29. Block, C., Janknecht, R., Herrmann, C., Nassar, N. & Wittinghofer, A. Quantitative structure-activity analysis correlating Ras/Raf interaction *in vitro* to Raf activation *in vivo*. *Nature Struct. Biol.* **3**, 244–251 (1996).
30. Hu, C.-D. *et al.* Cysteine-rich region of Raf-1 interacts with activator domain of post-translationally modified Ha-Ras. *J. Biol. Chem.* **270**, 30274–30277 (1995).
31. Drugan, J.K. *et al.* Ras interaction with two distinct binding domains in Raf-1 may be required for Ras transformation. *J. Biol. Chem.* **271**, 233–237 (1996).
32. Nur-E-Kamal, M.S.A. & Maruta, H. The role of Gln^{61} and Glu^{63} of *ras* GTPases in their activation by NF1 and ras GAP. *Mol. Biol. Cell* **3**, 1437–1442 (1992).
33. White, M.A. *et al.* Multiple Ras functions can contribute to mammalian cell transformation. *Cell* **80**, 1–20 (1995).
34. Joneson, T., White, M.A., Wigler, M.H. & Bar-Sagi, D. Stimulation of membrane ruffling and MAP kinase activtion by distinct effectors of RAS. *Science* **271**, 810–812 (1996).
35. Akasaka, K. *et al.* Differential structural requirements for interaction of Ras protein with its distinct downstream effectors. *J. Biol. Chem.* **271**, 5353–5360 (1996).
36. Amano, M. *et al.* Identification of a putative target for Rho as the serine-threonine kinase protein kinase N. *Science* **271**, 648–659 (1996).
37. Nonaka, H. *et al.* A downstream target of *RHO1* small GTP-binding protein is *PKC1*, a homolog of protein kinase C, which leads to activation of the MAP kinase cascade in *Saccharomyces cerevisiae*. *EMBO J.* **14**, 5931–5938 (1995).
38. Diekmann, D., Nobes, C.D., Burbelo, P.D., Abo, A. & Hall, A. Rac GTPase interacts with GAPs and target proteins through multiple effector sites. *EMBO. J.* **14**, 5297–5305 (1995).
39. Dorseuil, O., Reibel, L., Bokoch, G.M., Camonis, J. & Gacon, G. The Rac target NADPH oxidase p67^{phox} interacts preferentially with Rac2 rather than Rac1. *J. Biol. Chem.* **271**, 83–88 (1996)
40. Herrmann, C., Martin, G. & Wittinghofer, A. Quantitative analysis of the complex between p21^{ras} and the Ras-binding domain of the human Raf-1 protein kinase, *J. Biol. Chem.* **270**, 2901–2905 (1995).
41. Kabsch, W. Automatic processing of rotation diffraction data from crystals of initially unknown symmetry and cell constants. *J. Appl. Crystallogr.* **26**, 795–800 (1993).
42. Brünger, T.A. XPLOR version 3.1, Manual, Yale Univ. (1993).
43. Jones, T.A., Zou, J.Y., Cowan, S.W. & Kjeldgaard, M. Improved methods for binding protein models in electron density maps and the location of errors in these models. *Acta Crystallogr.* A**47**, 110–119 (1991).
44. Luzzati, P.V. Traitements statistique des erreurs dans la détermination des structures cristallines. *Acta Crystallogr.* **5**, 802–810 (1952).
45. Read, R.J. Improved Fourier coefficients for maps using phases from partial structures with errors. *Acta Crystallogr.* A**42**, 140–149 (1986).
46. Laskowski, R.A., MacArthur, M.W., Moss, D.S. & Thornton, J.M. PROCHECK: a program to check the stereochemical quality of protein structures. *J. Appl. Crystallog.* **26**, 283–291 (1993).
47. Nicholls, A., Sharp, K.A. & Honig, B. Proteinfolding and association: insights from the interfacial and thermodynamic properties of hydrocarbons. *Proteins Struct. Funct. Genet.* **11**, 281 (1991).